

defect sites,<sup>1,2,6,7,11,27,28,34-39</sup> and since Xe<sup>+</sup>-ion bombardment produces a greater concentration of defects at the surface, Xe<sup>+</sup>-ion-bombarded GaAs exhibits a greater enhancement of surface oxidation. Lighter ions impart defects deep into the crystal, and therefore the concentration of defects (sites for reactions) at the surface is smaller and there is less enhancement in the reactivity. Also, any damage present far from the surface (the first few atomic layers) may be of a different form. Defects on the surface may be composed mainly of broken Ga-As bonds with many singly occupied Ga dangling bonds (see Figure 10), while deeper defects may have a chance to re-form bonds within the bulk and thus form unreactive centers.

### Conclusions

The effect of bombarding ion mass on the chemical reactivity of GaAs was investigated for 3-keV <sup>3</sup>He<sup>+</sup>, Ne<sup>+</sup>, Ar<sup>+</sup>, and Xe<sup>+</sup> ions (constant fluence). Exposure of ion-bombarded GaAs surfaces to 10<sup>7</sup>-10<sup>11</sup> langmuirs of O<sub>2</sub> produced Ga<sub>2</sub>O<sub>3</sub>, As<sub>2</sub>O<sub>3</sub>, and As<sub>2</sub>O<sub>5</sub> with the preferential formation of Ga<sub>2</sub>O<sub>3</sub>, and exposure to 10<sup>13</sup> langmuirs of H<sub>2</sub>O yielded both GaO(OH) and Ga(OH)<sub>3</sub>. The greatest amount of oxidized gallium was found following exposure of 3-keV Xe<sup>+</sup>-ion-bombarded GaAs to O<sub>2</sub> or H<sub>2</sub>O. Comparison of the relative quantities of oxidized gallium

formed on ion-bombarded GaAs to that formed on chemically cleaned or IHT-prepared GaAs supports the conclusion that reactions take place at defect sites that are formed by ion bombardment. Since the greatest reactivity was observed for Xe<sup>+</sup>-ion-bombarded GaAs, this suggests that the greatest concentration of defects was present on a surface bombarded with Xe<sup>+</sup>.

The damage caused by ion bombardment was investigated by optical reflectivity in the visible and near-ultraviolet region (1.6-5.6 eV), by Raman spectroscopy, and by current-voltage and capacitance-voltage measurements. Ion bombardment was shown to form a structurally damaged layer as evidenced by the destruction of the peaks due to crystalline GaAs in the optical reflectivity and Raman spectra, and from these spectra it could be determined that the depth of ion-bombardment damage was inversely related to the mass of the bombarding ion. A similar depth versus mass relationship was indicated by the capacitance-voltage measurements. The overall capacitance of ion-bombarded GaAs decreased as a function of decreasing ion mass. However, all of the ion bombardments resulted in measurable changes in diode electrical parameters, with the severity of the change decreasing with increasing ion mass. The findings of this study suggest possible ways to modify the surface of GaAs, with smaller damage depths occurring for bombardment with ions of heavier mass.

**Acknowledgment.** We acknowledge the funding of this project by Texas Instruments, the Virginia Center for Innovative Technology, and the National Science Foundation (via an equipment grant). We also thank Frank Cromer for his help with the surface analysis equipment.

**Registry No.** GaAs, 1303-00-0; <sup>3</sup>He<sup>+</sup>, 15644-29-8; Ne<sup>+</sup>, 14782-23-1; Ar<sup>+</sup>, 14791-69-6; Xe<sup>+</sup>, 24203-25-6; H<sub>2</sub>O, 7732-18-5.

(34) Barton, J. J.; Goddard III, W. A.; McGill, T. C. *J. Vac. Sci. Technol.* **1979**, *16*, 1178.

(35) Spicer, W. E.; Chye, P. W.; Garner, C.; Lindau, I.; Pianetta, P. *Surf. Sci.* **1979**, *86*, 763.

(36) Ranke, W.; Jacobi, K. *Surf. Sci.* **1979**, *81*, 504.

(37) Bartels, F.; Mönch, W. *Surf. Sci.* **1984**, *143*, 31.

(38) Bartels, F.; Surkamp, L.; Clemens, H. J.; Mönch, W. *J. Vac. Sci. Technol. B* **1983**, *1*, 756.

(39) Mark, P.; Chang, C.; Creighton, W. F.; Lee, B. W. *CRC Crit. Rev. Solid State Mater. Sci.* **1975**, *5*, 189.

## Aromatic Hydrocarbon Intercalates: Synthesis and Characterization of Iron Oxychloride Intercalated with Perylene and Tetracene

Joseph F. Bringley<sup>†</sup> and Bruce A. Averill\*

Department of Chemistry, University of Virginia, Charlottesville, Virginia 22901

Received October 12, 1989

The reaction of a series of polycyclic aromatic hydrocarbons with the layered host FeOCl has been examined. Arenes with ionization potentials  $\leq$ ca. 7 eV react with FeOCl via an intercalation process. The intercalation compounds FeOCl(perylene)<sub>1/9</sub> and FeOCl(tetracene)<sub>1/12</sub> have been characterized. Powder X-ray diffraction studies of microcrystalline powders and oriented films of these materials indicate that in each case the guest molecules are oriented with their molecular planes perpendicular to the layers of the host lattice. FTIR spectra indicate that intercalation of these molecules into FeOCl occurs via a redox mechanism, in which approximately one electron is transferred to the host lattice per guest molecule. Temperature dependent conductivity measurements show a 10<sup>5</sup>-fold increase in conductivity over that of unintercalated FeOCl, with apparent bandgaps of 0.29 and 0.27 eV for the perylene and tetracene intercalates, respectively.

### Introduction

The lamellar transition-metal oxyhalides (MOX: M = Ti, V, Cr, X = Cl, Br; M = Fe, X = Cl) are able to undergo intercalation reactions that involve the reversible insertion of guest species (i.e., atoms or molecules) between infinite

two-dimensional sheets of the host. The host layers expand to accommodate the preferred orientation of the guest, as interlayer host-host interactions are replaced by more favorable host-guest and guest-guest interactions. Only relatively minor changes in the host structure accompany the intercalation process.<sup>1-4</sup> Among the layered

<sup>†</sup> Present address: IBM Research Division, Thomas J. Watson Research Center, Yorktown Heights, NY 10598.

\* To whom correspondence should be addressed.

(1) Halbert, T. R. In *Intercalation Chemistry*; Whittingham, M. S., Jacobson, A. J., Eds.; Academic Press: New York, 1982; Chapter 12.

MOX materials, an extensive intercalation chemistry is best established for FeOCl. A wide variety of atoms and molecules, including alkali metals (e.g., Li, Na, K), amines, amides, metallocenes, and various heteroaromatic molecules can be intercalated into these materials.<sup>1</sup> The rate of intercalation depends upon a number of factors, including the available host surface area, the solubility of the guest, the basicity of the solvent, and the purity of the host. These factors can be adequately controlled experimentally by, e.g., sonication of the pristine host to obtain a very finely divided starting material, appropriate choice of solvent, and careful assessment of the purity of the starting materials.

In addition to these factors, virtually all intercalation reactions of FeOCl are known to proceed with some degree of charge transfer from the guest to the host; the rate of reaction is therefore highly dependent upon the reduction potential of the guest species.<sup>3</sup> Intercalation into FeOCl does not occur if the guest is not a sufficiently good electron donor. For the layered host TaS<sub>2</sub>, intercalation has been shown to be dependent upon the reducing power of the guest; for example, cobaltocene (IP = 5.56 eV) intercalates readily into TaS<sub>2</sub>, whereas ferrocene (IP = 6.88 eV) does not.<sup>5</sup> However, no such data have been reported for FeOCl.

Polycyclic aromatic hydrocarbons (arenes) were chosen as potential guests for the following reasons: (i) many are relatively strong electron donors; (ii) their reduction and ionization potentials have been extensively studied;<sup>6,7</sup> (iii) a number of arenes, including perylene, pyrene, and fluoranthene, are known to form conducting materials with various electron acceptors.<sup>17-20</sup> Thus, they provide an accessible series of materials with which to study intercalation into FeOCl as a function of the reducing power of the guest species.

In addition, a continuing goal of research in this laboratory has been to demonstrate the use of layered intercalation hosts as macroanionic electron acceptors for the synthesis of low-dimensional organic conductors. This strategy involves the insertion of the organic donor molecules used for form organic conductors between the layers of inorganic hosts, forming stacks of potentially conducting organic donors separated by inorganic layers. The intercalation process intrinsically enforces the formation of the segregated donor-acceptor structure necessary to produce metallically conducting materials. Chemical modification of the host or guest species can then be used to control the amount of charge transfer, which is of paramount importance to the synthesis of organic conductors. This approach may provide a number of advantages over other methods, as discussed previously.<sup>8</sup> To date, such work has been limited to the intercalation of tetrathiafulvalene (TTF)<sup>9</sup> and related tetrathioles,<sup>10-12</sup> tetraselenafulvalene

and tetramethylselenafulvalene,<sup>8</sup> and bis(ethylenedithio)tetrathiafulvalene<sup>13</sup> into FeOCl and the intercalation of TTF into V<sub>2</sub>O<sub>5</sub><sup>14</sup> and smectic clays.<sup>15</sup> In addition, a preliminary characterization of the aromatic hydrocarbon intercalate FeOCl(peryleno)<sub>1/9</sub> has been reported.<sup>16</sup> Herein, we describe the synthesis and characterization of the first aromatic hydrocarbon intercalates: FeOCl(peryleno)<sub>1/9</sub> and FeOCl(tetraceno)<sub>1/12</sub>.

### Experimental Section

FeOCl was prepared by reaction of Fe<sub>2</sub>O<sub>3</sub> with a slight excess of FeCl<sub>3</sub> in an evacuated, sealed Pyrex tube for 1 week, employing a temperature gradient of 370–340 °C. The black microcrystalline product was washed with acetone and dried in vacuo. The Fe/Cl ratio was checked by elemental analysis to assess the purity of the material. Perylene, azulene, tetracene, and anthracene were purchased (Aldrich Chemical Co.) and purified by recrystallization from toluene. Cycloheptatriene was purchased (Mallinckrodt Chemical Co.) and purified by distillation from molecular sieves. Pyrene, acenaphthalene, and phenanthrene were purchased (Aldrich Chemical Co.) and used as received. The intercalates were prepared by treating FeOCl with equimolar amounts of saturated solutions of the guests in dimethoxyethane (DME) at 85 °C for 10 days to 6 weeks. The specific conditions of the reactions are outlined in Table I. The resulting products were then washed (DME, CH<sub>2</sub>Cl<sub>2</sub>) and dried in vacuo. Finely divided FeOCl was obtained by sonication (50 W, 20 min) of the pristine host in dry toluene. All reactions and manipulations were performed under a dry nitrogen atmosphere. DME was distilled from CaH<sub>2</sub> just prior to use. Reactions involving cycloheptatriene were accomplished by treating FeOCl with 1.0 M solutions of cycloheptatriene in dry acetonitrile. Elemental analyses (Fe, Cl, C, and H) for the perylene and tetracene intercalates are consistent with the stoichiometries FeOCl(peryleno)<sub>1/9</sub> and FeOCl(tetraceno)<sub>1/12</sub>. Intercalation was confirmed for all materials by powder X-ray diffraction; the absence of the characteristic 7.917 Å in interlayer reflection of pristine FeOCl was used to verify complete intercalation.

A Guinier camera (Enraf Nonius Model FR 552) equipped with a graphite monochromator to provide clean Cu Kα<sub>1</sub> radiation was employed to collect X-ray powder diffraction data photographically. Cell parameters were obtained by indexing the powder patterns with the least-squares program LATT<sup>22</sup> with FeOCl as a starting point. Oriented films of the intercalates were prepared by suspending the samples in chloroform and allowing the suspensions to dry on X-ray sample slides under an inert atmosphere. X-ray powder diffraction peak profiles of the oriented films were obtained on a Scintag XDS-2000 diffractometer. Structure factors were derived from integrated peak intensities and corrected for the Lorentz and polarization factors 1/sin 2θ and (1 + cos<sup>2</sup> 2θ)/2, respectively. The derived structure factors were phased by considering the scattering as a contribution of the FeOCl layers only. The signs of the phases were then checked by recalculation including the contribution of the guest molecules. To calculate

(12) Kauzlarich, S. M.; Ellena, J. F.; Stupik, P. D.; Reiff, W. M.; Averill, B. A. *J. Am. Chem. Soc.* **1987**, *109*, 4561.

(13) Bringley, J. F.; Fabre, J.-M.; Averill, B. A. Manuscript in preparation.

(14) Van Damme, H.; Letellier, M.; Tinet, D.; Kinel, B.; Ernc, R. *Mater. Res. Bull.* **1984**, *19*, 1635.

(15) Obrecht, F.; Letellier, M.; Van Damme, H. *Nouv. J. Chim.* **1984**, *8*, 681.

(16) Bringley, J. F.; Averill, B. A. *J. Chem. Soc., Chem. Commun.* **1987**, 399.

(17) Hoch, R.; Schweitzer, D.; Harms, R. H.; Keller, H. J.; Schafer, H.; Helberg, H. W.; Wilckens, R.; Geserich, H. P.; Ruppel, W. *Mol. Cryst. Liq. Cryst.* **1982**, *86*, 87.

(18) Kommandeur, J.; Hall, F. R. *J. Chem. Phys.* **1961**, *34*, 129.

(19) Kröhnke, C.; Enkelmann, V.; Wegner, G. *Angew. Chem., Int. Ed. Engl.* **1980**, *19*, 912.

(20) Keller, H. J.; Nöthe, D.; Pritzkow, H.; Weke, D.; Werner, M.; Harms, R. H.; Koch, P.; Schweitzer, D. *Chem. Scr.* **1981**, *17*, 101.

(21) Kikkawa, S.; Kanamaru, F.; Koizumi, M. *Bull. Chem. Soc. Jpn.* **1979**, *52*, 963.

(22) Takusagawa, F.; Corbett, J. D. Iowa State University, unpublished.

(23) Lind, M. D. *Acta Crystallogr.* **1972**, *B26*, 1058.

(2) Schöllhorn, R. *Pure Appl. Chem.* **1984**, *56*, 1739.

(3) Rouxel, J.; Palvadeau, P. *Rev. Chim. Mineral.* **1982**, *19*, 317.

(4) Levy, F. *Intercalated Layered Materials*; D. Reidel Press: Dordrecht, Holland, 1979.

(5) Jacobson, A. J. In *Intercalation Chemistry*; Whittingham, M. S., Jacobson, A. J., Eds.; Academic Press: New York, 1982; Chapter 7.

(6) Pysh, E. S.; Yang, N. C. *J. Am. Chem. Soc.* **1963**, *85*, 2124.

(7) Vendenev, V. I. In *Bond Energies, Ionization Potentials and Electron Affinities*; Price, W. C., Ed.; Scripta Technica: London, England, 1966; Chapter 3.

(8) Bringley, J. F.; Fabre, J.-M.; Averill, B. A. *Mol. Cryst. Liq. Cryst.* **1988**, *170*, 215.

(9) Antonio, M. R.; Averill, B. A. *J. Chem. Soc., Chem. Commun.* **1981**, 382.

(10) Kauzlarich, S. M.; Teo, B. K.; Averill, B. A. *Inorg. Chem.* **1986**, *25*, 28.

(11) Kauzlarich, S. M.; Stanton, J. L.; Faber, J. Jr.; Averill, B. A. *J. Am. Chem. Soc.* **1986**, *108*, 7946.

Table I. Reactions of Arenes with FeOCl

compound	$E_{1/2}$ , <sup>a,b</sup> V	IP, <sup>c</sup> eV	intercalation, <sup>d</sup> %	conditions <sup>e</sup>		
				solvt	temp, °C	time
cycloheptatriene		6.60	100	MeCN	60	10 days
azulene	0.71		dec	DME	60	14 days
tetracene <sup>f</sup>	0.77	6.6–6.8	100	DME	85	21 days
perylene	0.85	7.15	100	DME	85	21 days
anthracene <sup>f</sup>	1.09	7.4	NR	DME	85	6 weeks
pyrene <sup>f</sup>	1.16	7.5	NR	DME	85	6 weeks
acenaphthalene <sup>f</sup>	1.21		NR	DME	85	6 weeks
phenanthrene <sup>f</sup>	1.50	8.03	NR	DME	85	6 weeks

<sup>a</sup> Numbers are reduction potentials of monocation vs SCE. <sup>b</sup> Data from ref 6. <sup>c</sup> Data from ref 7. <sup>d</sup> NR = no reaction. <sup>e</sup> DME = dimethoxyethane, MeCN = acetonitrile. <sup>f</sup> Ionization potential of cycloheptatriene is that of the neutral radical cation. <sup>g</sup> Sonicated FeOCl used in reaction.

structure factors, the guest occupancy within the interlayer region was set at the value obtained from elemental analyses.

Fourier transform IR data were obtained on a Nicolet DX-5 spectrophotometer. Temperature-dependent resistivity measurements (300–77 K) were performed on microcrystalline powders of the intercalates pressed at ca. 2 kbar, using the standard dc four-terminal configuration with silver paint contacts to attach electrical leads. Current densities were typically 0.1 A/cm<sup>2</sup>.

### Results and Discussion

**Synthesis.** Table I lists the reduction and ionization potentials of various arenes and the conditions and results of their reactions with FeOCl. DME was chosen as the solvent for these reactions since it has been shown to facilitate intercalation reactions involving FeOCl, apparently by stabilizing the guest cations generated in the intercalation process.<sup>24</sup> The intercalation of various aromatic and heteroaromatic electron donors into FeOCl has been shown to occur via a redox mechanism.<sup>12</sup> In those cases where arene intercalation did not occur, other solvents, including tetrahydrofuran, acetonitrile, and toluene, were examined with the same result. Due to the extremely poor solubility of tetracene in DME, the rate of its intercalation into FeOCl is slow. The intercalation rate could be increased, however, by employing finely divided FeOCl as a starting material. This was obtained by sonication of the pristine host in dry toluene just prior to reaction. Complete intercalation of tetracene could then be achieved in ca. 3 weeks in dry DME at 85 °C. Finely divided FeOCl was used as a starting material for the reactions of the last four arenes listed in Table I. The enhancement of intercalation rate by ultrasound has been reported previously.<sup>25</sup> From Table I, it is clear that arenes with ionization potentials  $\leq 7.0$  eV intercalate into FeOCl readily, while anthracene, pyrene, etc., with higher ionization potentials, do not intercalate. Thus, the upper limit of the ionization potential for intercalation of a guest molecule into FeOCl appears to be 7.0–7.4 eV (limiting reduction potential of the corresponding cation, 0.86–1.09V). We also note that the heteroaromatic donors (e.g., TTF,  $E_{1/2} = 0.34$  V; TSF,  $E_{1/2} = 0.48$  V) previously intercalated into FeOCl have reduction potentials below these values.<sup>5,12,13</sup>

The strongest electron donor listed in Table I, cycloheptatriene, appears to intercalate into FeOCl. Some decomposition of the host lattice was always found to occur, however, as indicated by analyses that were consistently low in chlorine. The oxidation of cycloheptatriene to the tropylium cation involves the generation of a proton and two electrons. It is likely that the protons generated react with the chloride anions of the FeOCl layers to form

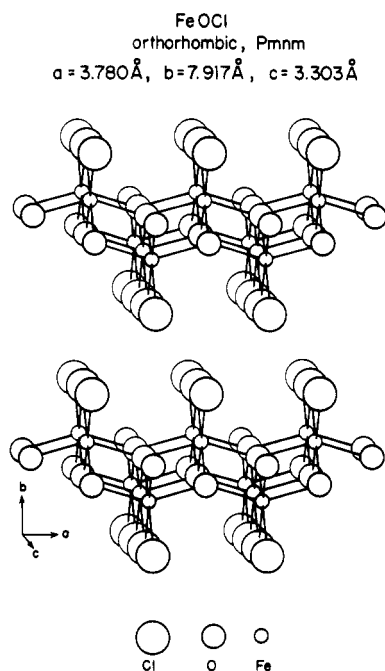


Figure 1. Illustration of two layers of the FeOCl structure (adapted from ref 1).

HCl, which can then cause further decomposition of the host lattice. FeOCl is known to be highly unstable in acidic media.<sup>1</sup> The reaction of azulene with FeOCl results in decomposition of the host lattice, for reasons that are not clear.

The reactions of perylene (PE) and tetracene (TET) with FeOCl result in the formation of the intercalates FeOCl(PE)<sub>1/9</sub> and FeOCl(TET)<sub>1/12</sub>, respectively. These materials represent the first aromatic hydrocarbon intercalates known. The guest species could be removed from these materials by prolonged extraction with polar solvents (e.g., DME), indicating the reversibility of the reaction and establishing these as true intercalation reactions. DME co-intercalates with perylene, resulting in the phase FeOCl(PE)<sub>1/9</sub>(DME)<sub>1/20</sub>. However, DME de-intercalates at lower temperatures (ca. 160–200 °C) than does perylene (ca. 300–400 °C) and could be selectively removed from the interlayer region of the host by heating in vacuo (190 °C, 10<sup>-2</sup> Torr, 2 days) with no significant changes in structural or physical properties. The inclusion of solvent molecules within crystals of (PE)<sub>2</sub>X salts has been reported previously.<sup>17,20</sup>

### Structural Studies

**FeOCl.** FeOCl crystallizes in the orthorhombic space group *Pmnm* with  $a = 3.780 \text{ \AA}$ ,  $b = 7.917 \text{ \AA}$ , and  $c = 3.303 \text{ \AA}$ .<sup>23</sup> The FeOCl structure (Figure 1) consists of double

(24) Schäfer-Stahl, H. *Synth. Met.* 1981, 4, 65.

(25) Chatakandu, K.; Green, M. L. H.; Thompson, M. E.; Suslick, K. S. *J. Chem. Soc., Chem. Commun.* 1987, 900.

(26) Bringley, J. F. Ph.D. Thesis, University of Virginia, 1989.

(27) Halbert, T. R.; Scanlon, J. C. *Mater. Res. Bull.* 1979, 14, 415.

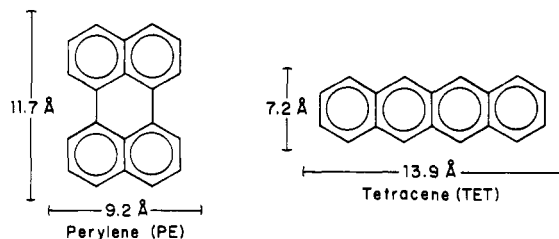


**Figure 2.** Schematic drawing illustrating the dimensions of the intercalants perylene (PE) and tetracene (TET).

layers of distorted, edge-shared  $\text{FeO}_{4/4}\text{Cl}_{2/2}$  octahedra, in which the chloride anions are cis-coordinated so that they are outermost on either side of the layers. Adjacent layers stack to form hexagonally close-packed sheets of chloride ions. Only relatively weak bonding interactions exist between the chloride layers, which is manifest by the number and variety of intercalates known for  $\text{FeOCl}$ .<sup>1</sup>

Extended X-ray absorption fine structure<sup>10</sup> and neutron powder diffraction studies<sup>11</sup> have shown that the Fe–O and Fe–Cl bonds of  $\text{FeOCl}$  are only slightly perturbed upon intercalation of tetrathiolenes such as TTF. The relative orientations of two adjacent layers, however, may change significantly upon insertion of a guest species.<sup>11,28</sup> This orientation is determined by the specific host–guest and guest–guest interactions of the intercalates, which result in a preferred orientation of the guest species.

**Intercalate Structure.** The X-ray powder diffraction patterns of the intercalates were indexed by using a body-centered unit cell with lattice parameters  $a = 3.782$  (2) Å,  $b = 3.321$  (1) Å, and  $c = 33.38$  (9) Å for  $\text{FeOCl}(\text{PE})_{1/9}$  and  $a = 3.773$  (10) Å,  $b = 3.311$  (10) Å, and  $c = 27.8$  (7) Å for  $\text{FeOCl}(\text{TET})_{1/12}$ . (The reflections observed in the diffraction data for all preparations of the latter were broad, suggesting a relatively low degree of order in this material.) Extinctions observed in the diffraction data for both materials could be accounted for by a doubling of the interlayer axis ( $c$ ). The packing of the chloride sheets consistent with a doubling of the interlayer axis and the systematic absences associated therewith have been discussed previously.<sup>11,28</sup> In each case the data are consistent only with a doubling of the  $c$  axis in which alternate  $\text{FeOCl}$  layers are shifted laterally by  $a/2$  and  $b/2$ , such that the chloride anions of adjacent layers are eclipsed. This model was first proposed by Halbert and Scanlon<sup>27</sup> for metalocene intercalates of  $\text{FeOCl}$  and appears to be quite general for  $\text{FeOCl}$  intercalates.<sup>8,10,11,13</sup>

Sixteen  $00l$  reflections were observed in the X-ray powder diffraction data of an oriented film of  $\text{FeOCl}(\text{PE})_{1/9}$  to  $d = 1.035$  Å. The interlayer distance calculated from these reflections is 16.65 (4) Å. The interlayer distance thus increases by approximately 8.7 Å upon intercalation. This expansion is only 0.5 Å less than the height<sup>29</sup> of the perylene molecule (Figure 2). It is consistent with an orientation of the perylene molecules perpendicular to the host layers but slightly interpenetrating the corrugated chloride sheets of  $\text{FeOCl}$ . An alternative model is a double layer of perylene molecules oriented with their molecular planes parallel to the layers. The latter model would, however, be expected to exhibit an increase in layer spacing of only 6.6–6.8 Å (twice the van der Waals thickness of the perylene aromatic ring), which is substantially less than that observed. The former alternative is therefore more plausible given this fact, the tendency of the perylene molecules to stack,<sup>17</sup> and the degree of interpenetration

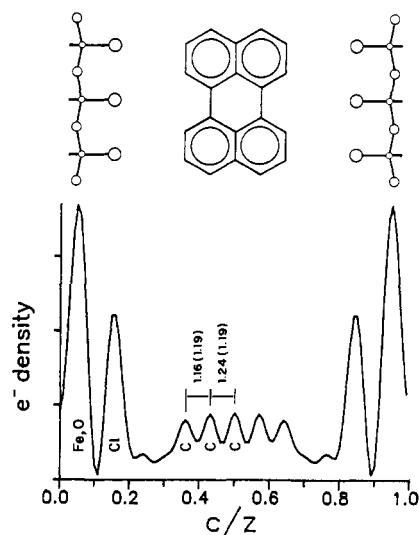


**Figure 3.** Bottom: projection of the electron density of  $\text{FeOCl}(\text{PE})_{1/9}$  along the interlayer axis. Top: illustration of the orientation of perylene as deduced from the electron density. Numbers are distances in angstroms calculated from the projection; numbers in parentheses are the corresponding distances calculated for the perylene molecule. Fe = small circles, O = medium circles, Cl = large circles.

into the  $\text{FeOCl}$  layers observed for many intercalates.

X-ray powder diffraction studies of microcrystalline powders provide a direct and accurate method of measuring interlayer distances in intercalated materials, from which relative host–host and host–guest orientations can be inferred. However, X-ray scattering is dominated by heavy atoms (i.e., the host layers); hence this method gives no direct information on the position or orientation of the guest species. Such information can be obtained, however, through X-ray powder diffraction studies of oriented microcrystalline films<sup>30–33</sup> of the intercalates. These films are well-ordered along the interlayer axis and hence the intensities of their interlayer  $00l$  reflections are significantly enhanced. A Fourier synthesis of the structure factors derived from the intensities can then be used to compute projections of the electron density of the intercalate along the interlayer axis. Atomic positions (0,0, $z$ ) can then be refined from the projections.<sup>34</sup>

A projection of the electron density along the interlayer axis of  $\text{FeOCl}(\text{PE})_{1/9}$  is shown in Figure 3 (bottom). The four interlayer peaks observed and their positions are readily assigned to distances within the perylene molecule. The data clearly show that the perylene molecules are oriented perpendicularly to the  $\text{FeOCl}$  layers; this model is represented schematically in Figure 3 (top). The distances from peak maxima are in excellent agreement with the corresponding distances observed in the perylene molecule.<sup>20</sup> This orientation is also consistent with that inferred from the X-ray powder diffraction data of microcrystalline samples of  $\text{FeOCl}(\text{PE})_{1/9}$ . The maximum stoichiometry calculated for perpendicularly oriented

(30) Nazar, L. F.; Jacobson, A. J. *J. Chem. Soc., Chem. Commun.* **1986**, 570.

(31) Maquire, J. A.; Benewicz, J. J. *Mater. Res. Bull.* **1984**, *19*, 1573.

(32) Kikkawa, S.; Kanamaru, F.; Koizumi, M. In *Reactivity of Solids*; Wood, Y., Lindquist, O., Vonneberg, A. N. G., Eds.; Plenum Press: New York, 1977; p 725.

(33) Ostani, S.; Shimada, M.; Kanamaru, I.; Koizumi, M. *Inorg. Chem.* **1981**, *19*, 1249.

(34) The reliability of the Fourier method depends strongly on the assumption that the signs of the phases are determined by the scattering of the  $\text{FeOCl}$  layers only. For  $\text{FeOCl}(\text{PE})_{1/9}$ , inclusion of the guest molecules in the model resulted in no changes in the signs of the phases, indicating the validity of the assumption.

(28) Phillips, J. E.; Herber, R. H. *Inorg. Chem.* **1986**, *25*, 3081.

(29) Distances calculated from ref 20.

close-packed perylene molecules is  $\text{FeOCl}(\text{PE})_{1/8}$ , which indicates that the perylene molecules are very nearly close-packed in  $\text{FeOCl}(\text{PE})_{1/9}$ .

As determined from X-ray powder diffraction data, the interlayer distance of 14.29 Å for  $\text{FeOCl}(\text{TET})_{1/12}$  represents an increase of 6.4 Å over that of pristine  $\text{FeOCl}$ . This expansion is only 0.8 Å less than the height of the tetracene molecule (Figure 2) and is again consistent with the guest molecules oriented perpendicular to the host layers (along the 7.2-Å dimension of tetracene; see Figure 2). However, the interlayer expansion of 6.6–6.8 Å expected for the double-layer model (discussed earlier) is also in agreement with that observed (6.4 Å). The maximum possible stoichiometries calculated for close-packed tetracenes in these models are  $\text{FeOCl}(\text{TET})_{1/10}$  and  $\text{FeOCl}(\text{TET})_{1/8}$ , respectively. The observed stoichiometry is more consistent with the former model; fitting the observed stoichiometry to the latter model would require that a significant number of vacant guest sites be present within the interlayer region of  $\text{FeOCl}$ , and no molecular intercalates are known in which ordered empty space is present in the interlayer region.<sup>35</sup> Based on these data alone, however, it is not possible to reach a definite conclusion regarding the orientation of the tetracene guest species. Projections of the electron density along the interlayer axis could not be obtained for this intercalate, since X-ray powder diffraction of oriented films of  $\text{FeOCl}(\text{TET})_{1/12}$  did not provide sufficient enhancement of the 00*l* reflections.

### Electronic Studies

Determining the degree of charge transfer from donor to acceptor is a problem of primary importance in the study of organic conductors. A major requisite for metallic conductivity in these systems is that there be a partial degree of charge transfer from donor to acceptor.<sup>36</sup> To determine the degree of charge transfer in the intercalates and hence to evaluate the feasibility of this method as a route to new low-dimensional organic conductors, we have examined the infrared spectra of these materials. These results are also of relevance in assessing the validity of the proposed redox mechanism of intercalation for these materials.

**FTIR Spectroscopy.** Infrared spectroscopy has been employed previously to elucidate the degree of charge transfer and charge distribution in organic conductors.<sup>37–39</sup> It has been shown that when the radical cations of organic conductors are present, intense new vibrational bands appear in the IR region.<sup>40</sup> This phenomenon, known as electron–molecular vibrational or “vibronic” coupling, is a result of intensity borrowing from electronic charge-transfer transitions. In the case of organic conductors, the presence of these bands has been interpreted in terms of a vibronic coupling of radical cation dimers, indicating a significant dimerization of the organic donor stacks. The energies (i.e., observed frequency shifts) of these vibronic bands are, in many cases, linearly related to the degree of oxidation of the donor stacks. Thus, it is possible to de-

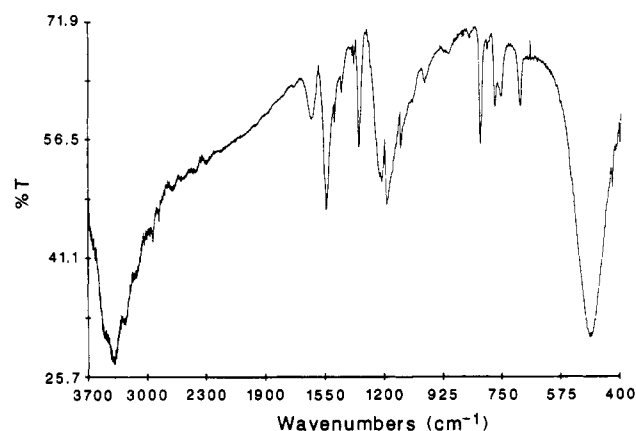


Figure 4. Infrared spectrum of  $\text{FeOCl}(\text{PE})_{1/9}$  in the region 3700–400  $\text{cm}^{-1}$ .

Table II. Infrared Spectral Features of Perylene,  $2\text{PE} \cdot 3\text{I}_2$ , and  $\text{FeOCl}(\text{P/E})_{1/9}$ <sup>a</sup>

perylene	$2\text{PE} \cdot 3\text{I}_2$	$\text{FeOCl}(\text{PE})_{1/9}$
3052 m	2927 w	2920 w
1605 m	2856 w	2849 w
	1541 s, br	1541 s, br
1592 m	1492 w	1496 w
1380 s	1386 w	
1335 m	1354 ms	1348 ms
1212 m	1219 ms	1219 ms
1186 m	1186 s	1186 s
1147 m		
	1110 w	1103 m
813 vs	813 m	819 m
767 vs	774 m	774 m
	750 w	754 m
	696 m	696 m
542 m	542 w	

<sup>a</sup> Frequencies are in wavenumbers ( $\text{cm}^{-1}$ ); relative intensities are indicated.

termine experimentally the degree of charge transfer in organic conductors using IR spectroscopy. Furthermore, the intensities of vibronic transitions are proportional to the degree of dimerization of the organic donor stacks, and hence provide information concerning the charge distribution within the stacks. Vibronic absorptions are of medium intensity in metallic (partially oxidized) organic conductors and are further washed out by low-lying electron absorptions.<sup>40</sup>

The FTIR spectrum of  $\text{FeOCl}(\text{PE})_{1/9}$  is shown in Figure 4. The strong absorptions at ca. 490  $\text{cm}^{-1}$  and the weaker absorption at 1630  $\text{cm}^{-1}$  are due to the  $\text{FeOCl}$  matrix. The remaining absorptions are nearly identical in frequency and in band shape to those observed in the FTIR spectrum of the conducting salt  $2\text{PE} \cdot 3\text{I}_2$ .<sup>18</sup> The strong, broad asymmetric absorptions observed at 1541, 1219, and 1186  $\text{cm}^{-1}$  are very likely of vibronic origin; this band shape is very typical of vibronic absorptions.<sup>37,39</sup> The presence of vibronic bands in the IR spectra of organic charge-transfer salts has been interpreted in terms of a dimerization of the organic donors. Furthermore, the positions and intensities of these absorptions have been shown to be proportional to the degree of oxidation.<sup>40</sup> Fully oxidized organic systems give rise to strong vibronic absorptions, while partially oxidized, metallic salts give broad, weak absorptions. The IR spectrum of  $\text{FeOCl}(\text{PE})_{1/9}$ , however, does not show the continuous broad absorptions in the region 4000–2000  $\text{cm}^{-1}$  as observed for the conducting salts. This is consistent with the semiconducting behavior observed for  $\text{FeOCl}(\text{PE})_{1/9}$  (see below). IR data for perylene,  $2\text{PE} \cdot 3\text{I}_2$  and  $\text{FeOCl}(\text{PE})_{1/9}$  are compared in Table II. The spectral

(35) Whittingham, M. S. In *Intercalation Chemistry*; Whittingham, M. S., Jacobson, A. J., Eds., Academic Press: New York, 1982; Chapter I.

(36) Wudl, F. *Acc. Chem. Res.* **1987**, *17*, 227.

(37) Bozio, R.; Zanon, I.; Girlando, A.; Pecile, C. *J. Chem. Phys.* **1975**, *71*, 2282.

(38) Meneghetti, M.; Bozio, R.; Zanon, I.; Pecile, C.; Ricotta, C.; Zannetti, M. *J. Chem. Phys.* **1984**, *80*, 6210.

(39) Chappell, J. S.; Bloch, A. N.; Bryden, W. A.; Maxfield, M.; Poehler, T. O.; Cowan, D. O. *J. Am. Chem. Soc.* **1981**, *103*, 2442.

(40) Bozio, R.; Pecile, C. In *The Physics and Chemistry of Low-Dimensional Solids*; Alcácer, L., Ed.; D. Reidel Press: Dordrecht, Holland, 1980; pp 165–186.

**Table III. Infrared Spectral Features of Tetracene and FeOCl(TET)<sub>1/12</sub><sup>a</sup>**

tetracene	character <sup>b</sup>	FeOCl(TET) <sub>1/12</sub>
3047 s	C-H str	3042 w
1632 m	ring str	1625 s
1542 m	ring str	1536 m
1466 s	ring str	1491 m, 1469 sh
1298 s	ring str	1324 m, br
1164 m	C-H in-plane bending	1296 m, br
1123 m	C-H in-plane bending	1187 w
995 m	C-H in-plane bending	1113 m, vbr
957 s	C-H out-of-plane bending	964 w
905 vs	C-H out-of-plane bending	919 m
743 vs	C-H out-of-plane bending	751 m
472 m	skeletal deform	700 m

<sup>a</sup>Frequencies are in wavenumbers (cm<sup>-1</sup>); relative intensities are indicated. <sup>b</sup>Data from ref 40; character reported is for tetracene vibrations only.

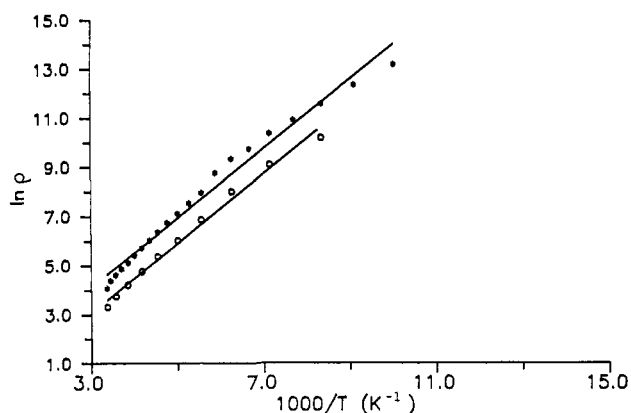


**Figure 5.** Temperature-dependent resistivity of the intercalates FeOCl(PE)<sub>1/9</sub> (stars) and FeOCl(TET)<sub>1/12</sub> (open circles) shown as  $\ln \rho$  versus  $1/T$ .

features match closely in both energy and intensity only for the peaks at 1186, 813, and 767 cm<sup>-1</sup> (for perylene). These absorptions are characterized by C-H in-plane and out-of-plane bending<sup>41</sup> and are expected to be relatively unaffected by ionization.<sup>40</sup> The above data clearly show that the perylene molecules are oxidized during the intercalation process but do not allow a precise estimation of the degree of charge transfer.

The FTIR spectral features of tetracene and FeOCl(TET)<sub>1/12</sub> are listed in Table III. The bands of FeOCl(TET)<sub>1/12</sub> are clearly different in both frequency and intensity from those of tetracene.<sup>41</sup> Furthermore, the FTIR spectrum of FeOCl(TET)<sub>1/12</sub> displays broad asymmetric absorptions and "antiresonance dips" typical of vibronic interactions in the 1700–900-cm<sup>-1</sup> region. These observations are consistent with an oxidation of the tetracene molecules during the intercalation process, although it is difficult to determine the specific degree of oxidation of the tetracene guests from these data alone.

**Conductivity.** Because single crystals could not be obtained from the intercalation reactions, conductivity measurements were performed on powdered samples of the intercalates that had been pressed at ca. 2 kbars. The resistivities of FeOCl(PE)<sub>1/9</sub> and FeOCl(TET)<sub>1/12</sub> are plotted as a function of temperature in Figure 5. These materials are semiconductors with bandgaps of 0.29 and 0.27 eV, respectively. The room-temperature conductivities are  $1.72 \times 10^{-2}$  (Ω cm)<sup>-1</sup> for FeOCl(PE)<sub>1/9</sub> and  $3.67 \times 10^{-2}$  (Ω cm)<sup>-1</sup> for FeOCl(TET)<sub>1/12</sub>. These values represent

**Table IV. Structural and Physical Properties of FeOCl and Intercalates**

property	FeOCl	FeOCl(PE) <sub>1/9</sub>	FeOCl(TET) <sub>1/12</sub>
interlayer dist, Å	7.917	16.65 (4)	14.29
interlayer expansion, Å		8.7	6.4
nesting, <sup>a</sup> Å		0.5	0.6
charge transfer		5.1	5.1
$\sigma_{RT}$ , (Ω cm) <sup>-1</sup>	10 <sup>-7</sup>	ca. 1.0?	ca. 1.0?
bandgap, eV	0.61	0.29	0.27

<sup>a</sup>Nesting refers to the interpenetration of the guest species into the host lattice.

a  $10^5$  (Ω cm)<sup>-1</sup> increase in conductivity over that of pristine FeOCl, for which  $\sigma_{RT} = 1 \times 10^{-7}$  (Ω cm)<sup>-1</sup>. Little can be concluded, however, regarding the origin of the increased conductivity, since increases in conductivity of  $10^3$ – $10^4$  (Ω cm)<sup>-1</sup> are typically observed for intercalates of FeOCl. The conductivity of FeOCl has been attributed to a hopping mechanism within the FeOCl layers;<sup>42</sup> thus, the increase in conductivity may be due to the electrons added to the host upon oxidation of the guest molecules and not originating from the organic layers.

### Conclusions

A study of the intercalation of arenes into the layered host FeOCl has led to the synthesis of the intercalates FeOCl(PE)<sub>1/9</sub> and FeOCl(TET)<sub>1/12</sub>. These materials represent the first hydrocarbon intercalates known. The upper limit for the ionization potential of the guest for successful intercalation into FeOCl has been established to be 7.15–7.4 eV; the corresponding upper limit of the guest cation reduction potential is 0.85–1.09 V. These data should allow other workers to screen potential guests as a function of their ionization (or reduction) potentials. However, these limits are influenced by other factors, including the solubility of the guest species and the basicity of the solvent used. It should be noted that many amines that are known to intercalate into FeOCl<sup>1</sup> have ionization potentials well above that established limit (e.g., NH<sub>3</sub>, IP ≈ 10.3 eV; pyridine, IP ≈ 9.3 eV).<sup>18</sup> However, on the basis of earlier reports,<sup>43,44</sup> it seems clear that while the intercalation of these molecules into FeOCl involves some degree of electron transfer to the host, the redox process is assisted by further reaction of the guest species during the intercalation process. For example, prolonged exposure of FeOCl to NH<sub>3</sub> results in topotactic substitution of the chloride anions of FeOCl to form FeONH<sub>2</sub> and NH<sub>4</sub>Cl.<sup>45</sup> The mechanism of intercalation of nitrogen-containing compounds into various layered materials is therefore apparently more complex, with possibilities such as coupling via N–N and C–C bond formation to be considered. Furthermore, the structures of nitrogen-containing intercalates are known to be strongly stabilized by N–H<sup>+</sup>---N dipole interactions.<sup>44,45</sup>

The structural and physical properties of the intercalates and FeOCl, for comparison, are summarized in Table IV. X-ray powder diffraction studies of both microcrystalline powders and oriented films of FeOCl(PE)<sub>1/9</sub> clearly show that the perylene molecules are oriented perpendicular to the host lattice. X-ray powder diffraction studies of microcrystalline powders of FeOCl(TET)<sub>1/12</sub> suggest that the

(42) Herber, R. H.; Eckert, H. *Phys. Rev. B* 1985, 31, 34.

(43) Schöllhorn, R.; Zagefka, H.-D. *Angew. Chem., Int. Ed. Engl.* 1977, 16, 199.

(44) Schöllhorn, R.; Zagefka, H.-D.; Butz, T.; Lerf, A. *Mater. Res. Bull.* 1979, 14, 369.

(45) Hagenmuller, P.; Rouxel, J.; David, J.; Colin, A.; LeNeindre, B. *Z. Anorg. Allg. Chem.* 1963, 323, 1.

(41) Codehnal, J.; Stepah, V. *Coll. Czech. Chem. Commun.* 1971, 36, 3981.

tetracene molecules are also aligned with their molecular planes perpendicular to the FeOCl layers. Thus, one requirement for metallic conductivity in organic conductors, namely, that the donors be crystallized in segregated stacks, has been achieved for these materials. The guest molecules are very nearly close packed within the interlayer region of FeOCl.

Strong vibronic absorptions are observed in the IR spectra of FeOCl(PE)<sub>1/9</sub> and FeOCl(TET)<sub>1/12</sub>. The IR data for these materials show that charge transfer from guest to host occurs during the intercalation process and that the guest species may be present as radical cations within the FeOCl galleries. This is further borne out by the observed semiconducting behavior of the intercalates. The room-temperature conductivities of FeOCl(PE)<sub>1/9</sub> and FeOCl(TET)<sub>1/12</sub> are 10<sup>5</sup> greater than that of FeOCl, pre-

sumably due to the electrons added to the host lattice upon oxidation of the guest species. Current work in our laboratory is focused on developing methods for controlling the degree of charge transfer in these and related materials.

**Acknowledgment.** This work was supported in part by the National Science Foundation, Solid State Chemistry Grant DMR-8313252. We thank Dr. K. Manus Wong for the measurement of temperature-dependent conductivity data and Dr. J.-M. Fabre, T. E. Sutto, and Dr. R. F. Bryan for helpful discussions.

**Supplementary Material Available:** Elemental analysis and X-ray diffraction data for the intercalates, and FTIR spectrum of FeOCl(TET)<sub>1/12</sub> (3 pages);  $F(\text{obs})$  vs  $F(\text{calc})$  for FeOCl(PE)<sub>1/9</sub> (1 page). Ordering information is given on any current masthead page.

## X-ray Photoelectron Spectroscopy Studies of Solvated Metal Atom Dispersed Catalysts. Monometallic Iron and Bimetallic Iron-Cobalt Particles on Alumina

Beng Jit Tan, Kenneth J. Klabunde,\* and Peter M. A. Sherwood\*

Department of Chemistry, Willard Hall, Kansas State University, Manhattan, Kansas 66506

Received October 19, 1989

XPS studies of solvated metal atom dispersed (SMAD) catalysts coupled with detailed studies of reference compounds of iron metal, FeO, Fe<sub>2</sub>O<sub>3</sub>, Fe<sub>3</sub>O<sub>4</sub>, and FeOOH were carried out. It is shown that toluene-solvated iron atoms nucleate at surface OH groups of the Al<sub>2</sub>O<sub>3</sub> catalyst support. The resultant iron oxide surface species served as nucleation sites for deposition of more iron atoms, leading to very small metallic iron clusters/particles. A thin oxide layer was detected on the particle surface that is believed to come from adventitious oxygen. When toluene-solvated cobalt and iron atoms were allowed to mix and nucleate together, iron reacted with and deposited on surface OH groups first. Then nucleation of Co and Fe occurred together on these surface iron oxide sites, with a slight excess of iron on the inside part of the particle. The iron oxide served as a gradient between the ionic support oxide and metallic iron/cobalt. Mössbauer spectroscopy confirmed the metallic nature of SMAD iron particles (unsupported).

### Introduction

By using solutions of solvated metal atoms of limited thermal stability, we have been able to prepare very highly dispersed heterogeneous catalysts of Fe,<sup>1</sup> Co-Mn,<sup>2,3</sup> Ni,<sup>4</sup> Pt-Sn,<sup>5</sup> Pt-Re,<sup>6</sup> and other metallic particles on various catalyst supports.<sup>7-9,11</sup> Bimetallic systems have proven particularly interesting, exhibiting remarkable catalytic activities where one metal can have a significant effect on the other. Those unusual properties stem from unique particle structures (e.g., cobalt layers on manganese),<sup>8</sup> high dispersion,<sup>9</sup> and the ability of one metal to behave sacrificially for the other.<sup>8</sup>

In this study we deal with iron-solvated metal atom dispersed (SMAD) catalysts and iron-cobalt combinations. This combination was chosen for their similar oxophilicity and stabilities as solvated atoms in toluene. We wished

to learn if such similar metals would yield alloy-like particles by the SMAD method or whether layered structures would result, with one metal acting sacrificially (being oxidized by support OH groups) to preserve the other in a nonoxidized, metallic state.<sup>10</sup>

### Experimental Section

**Materials.** Metals were obtained from Matheson, Coleman, and Bell (iron) and Cerac, Inc. (cobalt) in high purity forms. The support used was American Cyanamid  $\gamma$ -Al<sub>2</sub>O<sub>3</sub> (200 m<sup>2</sup>/g) and was calcined at 773 K for 3 h in flowing dry air (420 mL/min) and cooled in flowing nitrogen (500 mL/min). Purified deoxygenated toluene was used exclusively as the codeposition solvent for the metal atoms. Commercially available (Alfa Products) metals, metal oxides, and hydroxides were used as reference compounds.

**Catalyst Preparation.** The metal vapor reactor and catalyst preparation methods have been described earlier.<sup>4,5,9,12</sup> Metal loadings on Al<sub>2</sub>O<sub>3</sub> are given in the text and tables.

**XPS Experiments.** Sample preparation and handling have been described earlier.<sup>8a</sup> Our XPS measurements were made using an AEI ES200B spectrometer with a base pressure of better than

- (1) Kanai, H.; Tan, B. J.; Klabunde, K. J. *Langmuir* 1986, 2, 760.
- (2) Klabunde, K. J.; Imizu, Y. *J. Am. Chem. Soc.* 1984, 106, 2721.
- (3) Imizu, Y.; Klabunde, K. J. In *Catalysis of Organic Reactions*; Augustine, R. L., Ed.; Marcel Dekker: New York, 1985.
- (4) Matsuo, K.; Klabunde, K. J. *J. Catal.* 1982, 73, 216.
- (5) Li, Y. X.; Klabunde, K. J. *Langmuir*, 1987, 3, 558.
- (6) Ahkmedov, V.; Klabunde, K. J. *J. Mol. Catal.* 1988, 45, 193.
- (7) Klabunde, K. J.; Tanaka, Y. *J. Mol. Catal.* 1983, 21, 57, and references therein.
- (8) (a) Tan, B. J.; Klabunde, K. J.; Tanaka, T.; Kanai, H.; Yoshida, S. *J. Am. Chem. Soc.* 1988, 110, 5951. (b) Tan, B. J.; Klabunde, K. J.; Sherwood, P. M. A. *J. Am. Chem. Soc.*, submitted. (c) McIntyre, N. S.; Cook, M. G. *Anal. Chem.* 1975, 47, 1975.
- (9) Matsuo, K.; Klabunde, K. J. *J. Org. Chem.* 1982, 47, 843.

- (10) Woo et al. (Woo, S. J.; Godber, J.; Ozin, G. A. *J. Mol. Catal.* 1989, 52, 241 have very recently reported on the interaction of solvated iron atoms with silica O-H surface groups.

- (11) Li, Y. X.; Zhang, Y. F.; Klabunde, K. J. *Langmuir* 1988, 4, 385.
- (12) Klabunde, K. J.; Timms, P. L.; Skell, P. S.; Ittel, S. *Inorg. Synth.* 1979, 19, 59. Shriver, D. (editor) gives a general description of metal atom vapor chemistry.